Disconnection-mediated motion of ⟨110⟩ tilt grain boundaries in α-Fe

N. Kvashin, * N. Anento, and A. Serra
Department of Civil and Environmental Engineering, Universitat Politècnica de Catalunya, Barcelona 08034, Spain

(Received 23 March 2022; revised 3 May 2022; accepted 6 May 2022; published 31 May 2022)

It is possible for ⟨110⟩ tilt grain boundaries (GBs) in bcc metals to perform a conservative displacement by the glide of intrinsic GB line defects, namely, disconnections. The paper presents the characteristic of these defects in {112} and {332} twin boundaries, their vicinal GBs, and the {116} GB studied by molecular dynamics simulation. The sources of disconnections and their interaction with the other GB dislocations are described together with their role in the shear-coupled GB migration. The absence of gliding disconnections in the {111} GB impedes the shear-coupled GB migration, but two pure shuffles inside the coincident site lattice unit facilitate the transformation of the {111} GB into {110}/{001} or {110}/{112} facets in regions of concentration of stresses.

DOI: 10.1103/PhysRevMaterials.6.053607

I. INTRODUCTION

Metals and alloys are naturally polycrystalline, and their plastic response is defined by a number of physical processes involving intrinsic defects and the interactions between them. The main mechanism behind plastic deformation is the mobility of dislocations [1]. Therefore, the presence of obstacles hindering dislocation motion has, as a consequence, an effect on the mechanical response of the material. In simplified models used on early studies, grain boundaries (GBs) were considered as static obstacles [2]; however, technological advances in experimental techniques and computer modeling have evidenced that GB displacement is not negligible and it affects the interaction with other defects. In the special case of nanocrystalline materials, the grain size is small enough to suppress typical intragranular processes therefore GB migration becomes an alternative mechanism for plastic deformation [3–5]. Thus, macroscopic deformation is sustained by two processes, the first being the propagation of dislocations through grains, which is mediated by the interaction of dislocations with the GBs [6]. The second is the activation of several atomic processes intrinsic to the GBs: GB migration, formation of grain boundary dislocations (GBDs), nucleation of dislocations [7], and nucleation of twins [8].

Many experimental results [9,10] and molecular dynamics (MD) simulations [11] have evidenced that an efficient atomic mechanism involved in plastic deformation of metals at low temperature is the shear-coupled GB migration (SCGBM). The key element in this mechanism is a special type of interfacial defect which is glissile and shows both dislocation and step character, named disconnection. These defects are characterized by the Burgers vector (BV) and the height of the step (**b**, h) and, being glissile, they are responsible for the displacement of the GB. Recent computer atomistic studies in α-Fe [12–15] are examples of the importance of disconnections on the GB migration but also on the interaction between GBs and crystal dislocations. Another relevant finding is that in the event of glissile disconnection absence the plasticity mechanisms are not able to include SCGBM [16].

Among the many possible interfaces present in metals, tilt GBs are of special interest because they are frequently observed in experimental measurements [17,18], suggesting that they are energetically favored over other families of GBs. In the present paper we focus on four symmetric tilt GBs with a ⟨110⟩ tilt axis, which have been chosen to represent cases of special interest on the plasticity of bcc metals. The first two GBs considered are the $\Sigma3\{112\}\langle110\rangle$ and the $\Sigma11\{332\}\langle110\rangle$; both are coherent boundaries of the conjugate twin modes found in bcc materials, namely, {112} and {332} twins [19–22]. Glissile disconnections are observed in both boundaries, although, as we will detail below, the dynamic behavior of each interface is quite different. The third GB chosen is the $\Sigma3\{111\}\langle110\rangle$, which represents an extreme case: absence of mobile disconnections. This feature has many consequences on the response of this GB under externally applied shear stress, the most relevant of which being the inability to perform SCGBM. Finally, the fourth GB investigated is the $\Sigma19\{116\}\langle110\rangle$, which can be considered as an intermediate case: several disconnections are involved in the reactions from the GB-dislocation interaction and SCGBM is observed. This set of GBs covers a wide range of values for the misorientation angle and low Σ, allowing us to consider different structural units and enabling us to investigate in detail the role of GB atomic structure in the creation of glissile disconnections involved in the motion of the ⟨110⟩ tilt GBs.

To analyze the possible Burgers vectors of the GBDs we use the dichromatic pattern obtained by superimposing the lattice sites of the upper and lower crystals of a GB [23]. Any admissible GBD, the BV of which is depicted with an arrow in the dichromatic pattern, can be easily identified as it is related to the difference of broken symmetries of the two crystals forming the bicrystal [24–27]. The notation $\mathbf{b}_{n/m}$ has been adopted to refer to GBDs, as detailed in Ref. [12]. Among the GBDs, the glissile disconnections with BV parallel to the GB and with small values of (**b**, h) are named "elementary

*Corresponding author: nikolai.kvashin@upc.edu

 ©2022 American Physical Society

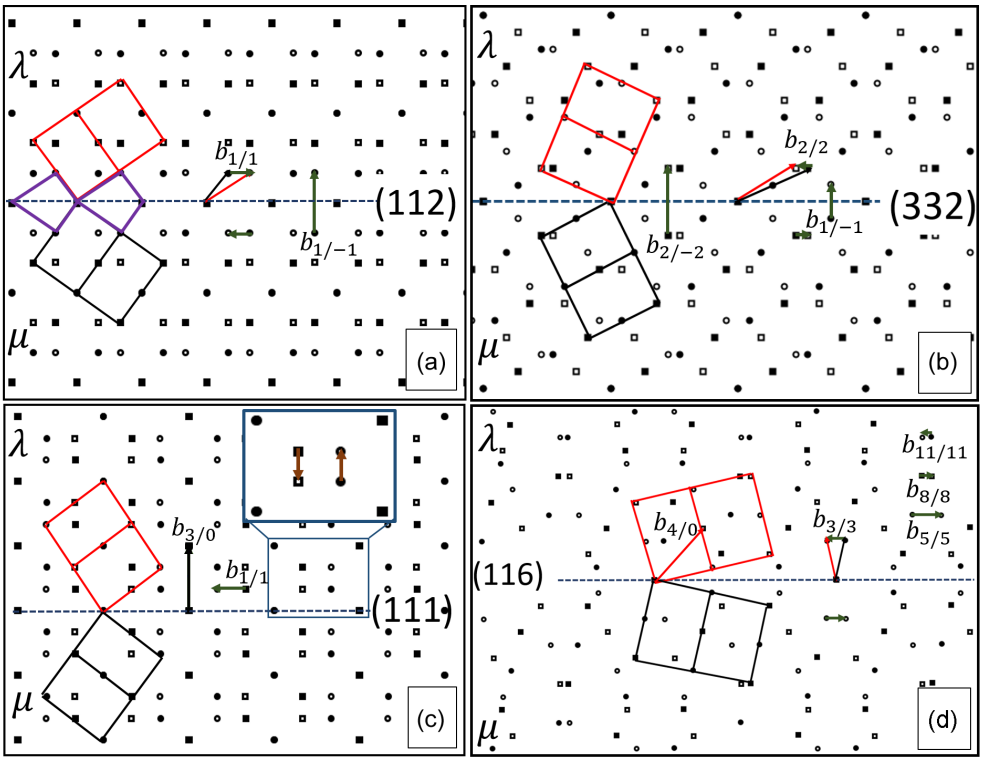

FIG. 1. [110] projections of the dichromatic pattern for the ⟨110⟩ symmetric tilt grain boundaries investigated including the GBDs involved in the reactions described.

disconnections" (EDisc). The EDisc show a high mobility and are responsible for the GB migration. The EDisc can be produced in several ways: (i) by nucleation of a dipole in the pristine interface, when the local shear stress exceeds a threshold value specific for each GB; (ii) as an outcome of the interaction between the GB and crystal dislocations; and (iii) generated by a GBD acting as a source of disconnections [12]. As the EDisc glide along the GB they can interact with other GBDs, affecting the motion of the EDisc. In Fig. 1 we represent all the EDisc observed for each GB, the properties of which are summarized in Table I.

In this paper we summarize in Sec. III the main trends of the {112}, {332}, and {111} GBs under an applied shear stress. We describe the properties of the GBs that are vicinal to the {112} and {332} GBs in Sec. IV. In Sec. V we report the behavior of the {116} GB as an example of the activation of several disconnections during deformation. Finally, in Sec. VI we present the concluding remarks.

TABLE I. Summary of the properties of the EDisc involved in SCGBM for each GB.

GB	$\mathbf{b}_{n/m}$	BV magnitude	ED height	CRSS (MPa)
{112}	$\mathbf{b}_{\pm1/\pm1}$	0.288 a_0	0.408 a_0	20
{332}	$\mathbf{b}_{\pm2/\pm2}$	0.302 a_0	0.426 a_0	550 and 620
{116}	$\mathbf{b}_{\pm3/\pm3}$	0.229 a_0	0.487 a_0	4000 and 4700
	$\mathbf{b}_{\pm5/\pm5}$	0.344 a_0	0.811 a_0	unstable
	$\mathbf{b}_{\pm8/\pm8}$	0.115 a_0	1.298 a_0	
	$\mathbf{b}_{\pm11/\pm11}$	0.115 a_0	1.784 a_0	

II. METHODOLOGY

A set of MD simulations on the ⟨110⟩ tilt GBs in α-Fe has been performed using the LAMMPS code [28]. The embedded-atom method potential developed by Ackland *et al.* [29] has been used to model the interatomic interactions in iron. The choice of this interatomic potential is based on its ability to reproduce accurately the properties of this family of GBs [30] and the properties of dislocation lines obtained from density functional theory as well. In the bicrystals constructed, the principal axes x, y, and z of the upper crystal (λ) are oriented perpendicular to the tilt axis and included into the GB, along the tilt axis and along the axis perpendicular to the interface, respectively, while for the lower crystal (μ) the orientation of the axes is mirror reflected. Periodic boundary conditions were imposed along the tilt axis and the axis along the GB interface, with fixed boundaries along the axis perpendicular to the interface. Approximate dimensions of the cell size range from 700 × 16 × 500 to 950 × 18 × 700 Å along the corresponding directions with the total number of atoms ranging from approximately 400 000 up to 700 000 atoms.

In order to investigate the possible mechanisms involving disconnections on the SCGBM, different setups have been employed: (i) a pristine interface, (ii) the GB interacting with a single dislocation, and (iii) the GB interacting with a dislocation pileup (DPU). The dislocations considered are pure edge gliding on {112} planes and mixed gliding on {110} planes. A fixed integration MD time step of 1 fs was used for all runs. For the first two setups an incremental shear strain is applied to the whole simulation box. This allows us either to initiate reactions at the pristine interface or to move the dislocation to

initiate the interaction with the interface. In simulations with nonzero temperature, a Nose-Hoover thermostat is used.

For the case of GB-DPU interaction a hybrid model combining atomistic and continuum approaches, initially described in Ref. [31] and applied in Refs. [13,15,16,32], has been employed. The heading dislocation of the DPU is placed in a few atomic planes from the interface. The positions of the following dislocations are calculated according to the expression $n = L\sigma/A$ [1]. Along with the increasing applied strain, the following dislocations enter the simulation box pushing the heading ones inducing reaction at the interface. Since the model uses the outer region of atoms to emulate strain application, periodic boundaries were only used along the tilt axis.

The stress state of the system is recorded after each increment of strain and the open visualization tool OVITO [33] is used for visualization and analysis of the atomic configuration. The common neighbor analysis provided allows us to construct Burgers circuits easily to derive the products of the reactions using dichromatic patterns. To understand the role of temperature in the disconnection production and interaction processes we have considered different simulation setups—quasistatic simulations (at $T = 0$ K) and dynamic simulations with nonzero temperature—thus enhancing or reducing the role played by thermal activation.

III. MAIN TRENDS OF {112}, {332}, AND {111} GRAIN BOUNDARIES

A. The {112} GB

The grain boundary $\Sigma3\{112\}\langle110\rangle$ presents several specific features endowing it with a relevant role in the plasticity mechanisms in bcc polycrystalline metals. As detailed before, it is the coherent boundary of the {112} twin which has been proven experimentally to effectively strengthen materials by impeding dislocation motion [34]. Another distinctive feature comes from the energetic analysis: Ref. [35] shows that this interface has the lowest grain boundary energy among all the symmetric tilt GBs. The grain boundary population is shown to be inversely correlated with the grain boundary energy [17], which explains why the symmetric {112} GB is the most frequently observed GB in bcc-Fe. Finally, the interfacial structure of this GB is a repetition of a simple structural unit, shown in Fig. 1(a), presenting a slightly distorted perfect crystal coordination.

The outcome of all the reactions observed with crystal dislocations is the creation of a GBD, identified in Fig. 1(a) as $\mathbf{b}_{1/-1}$ along with the emission of an ED, $\mathbf{b}_{1/1}$ (or the complementary $\mathbf{b}_{-1/-1}$) [12,15]. This disconnection has a short BV ($\approx 0.29a_0$); it steps the boundary only one plane ($h = 1$), which means that no shuffles are required during glide [36]; and it shows a high mobility due to a very low resolved shear stress ($\approx$ 20 MPa [37]). The GBD $\mathbf{b}_{1/-1}$ acts as a source of pairs of disconnections of opposite sign created on each side of the GBD, as shown in Fig. 2. This production process of EDisc can be sustained because the GBD moves together with the GB by a conservative climb [12] (see video 112 + 1D.mp4 in Supplemental Material [38]). The shear stress required to create a disconnection dipole in the pristine interface is around

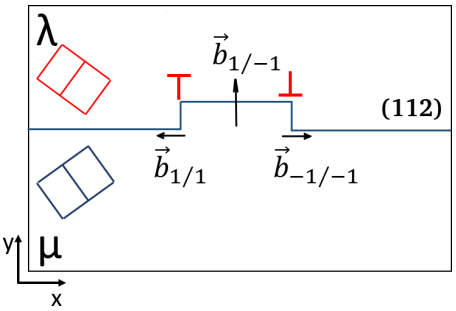

FIG. 2. Schematic showing the $\mathbf{b}_{1/-1}$ GBD acting as a source of ED dipoles.

2.4 GPa while for the source of disconnections the stress level required is lower, around 2 GPa, as shown in Fig. 3. Both disconnection production mechanisms contribute to the SCGBM.

B. The {332} GB

The second family of GBs investigated corresponds to the {332} tilt GB. Like for the previous case, only one type of EDisc is involved in the reactions observed, identified as $\mathbf{b}_{2/2}$ or $\mathbf{b}_{-2/-2}$ in the corresponding dichromatic pattern of Fig. 1(b). Likewise, this disconnection has a short BV (≈ 0.30 a_0) and it steps the boundary a similar height (≈ 0.43 a_0) but involving two (332) planes. Then, the resolved shear stress is higher ($\approx$ 550–620 MPa [14]) due to the necessary shuffles of the atoms in the disconnection core. These EDisc can be created in the pristine interface to initiate SCGBM (when shear stress is $\approx$ 1.45 GPa) but they can also be produced by a source of disconnections, the GBD $\mathbf{b}_{2/-2}$, capable to move together with the GB (see Fig. 5 in Ref. [14]).

Despite these similarities, there are significant differences associated to the reaction of the GB with crystal dislocations. In the {332} GB there are several types of GBDs produced as outcome, namely, $\mathbf{b}_{2/-2}$ and the disconnections $\mathbf{b}_{8/6}$, $\mathbf{b}_{10/8}$, $\mathbf{b}_{3/4}$, $\mathbf{b}_{-5/-6}$, $\mathbf{b}_{12/10}$, $\mathbf{b}_{-10/-12}$, $\mathbf{b}_{-12/-10}$, and $\mathbf{b}_{10/12}$ described in detail in Ref. [14]. The SCGBM is produced if the interaction of the EDisc and the GBDs performs a

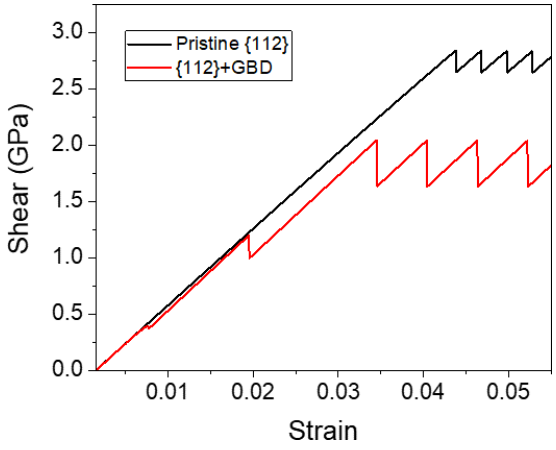

FIG. 3. Shear stress vs strain increment for the {112} GB pristine interface and interface containing a GBD.

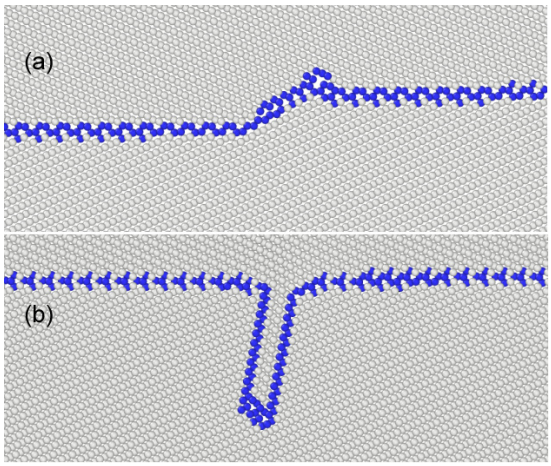

FIG. 4. Snapshots of MD simulation of a {332} GB with (a) a $\mathbf{b}_{8/6}$ GBD that moves along with the migrating interface and (b) a {112} twin produced as a result of interaction between EDisc and the sessile $\mathbf{b}_{-12/-10}$ GBD.

conservative climb, for instance the interaction with $\mathbf{b}_{8/6}$, shown in Fig. 4(a). Otherwise, the GBD stops the glide of the EDisc leading to the formation of {112} twins as in the interaction with $\mathbf{b}_{-12/-10}$, as shown in Fig. 4(b) and Fig. 6 in Ref. [14].

C. The {111} GB

The third GB considered has been the $\Sigma 3\{111\}\langle 110\rangle$, which is a symmetric tilt GB with a high-angle misorientation ($\Theta = 109.53^\circ$) and a high GB energy (≈ 1.3 J/m^2). The dichromatic pattern for this GB [Fig. 1(c)] shows that there is only one possible candidate of EDisc that could participate in the SCGBM, however neither this ED nor a different one appears in the results. Under shear stress loading, the pristine interface remains unchanged up to a very high stress level (≈ 9 GPa at $T = 0$ K). At this point a transformation of the interface is produced via the creation of pure steps without dislocation character. The steps are created by the shuffling of two atoms of the coincident-site lattice (CSL) unit cell [inset in Fig. 1(c)]. This is a shear-induced process with an energy barrier of 99 mJ/m^2 [16].

When a single $\mathbf{b}_{3/0}$ ($\mathbf{b}_{-3/0}$) dislocation shown in Fig. 1(c) glides towards the GB there is no absorption reported; it remains attached to the interface keeping its BV. However, this attached dislocation acts as a stress concentrator, allowing the formation of steps on the GB, but the external stress required is significantly lower (between 4 and 6.7 GPa). When interacting with a dislocation pileup of $\mathbf{b}_{3/0}$ ($\mathbf{b}_{-3/0}$) the local stress on the interaction region increases, enhancing the creation of steps and leading to the formation of a new interface containing {001}/{110} or {110}/{112} facets (Fig. 5). As a consequence of the formation of these facets the upper grain extends into the lower grain, however no GB migration takes place. The main conclusion from these observations is that stepping the interface is the mechanism on this GB to accommodate plastic deformation. Comparing the shear stress levels required to activate this mechanism (between 4 and 9 GPa) with those measured for the {112} GB (between 1.6 and 2.8 GPa) and the {332} GB (between 1.4 and 4.1 GPa) suggests that it is the least efficient of all and the {111} GB is an impenetrable obstacle for the glide of dislocations.

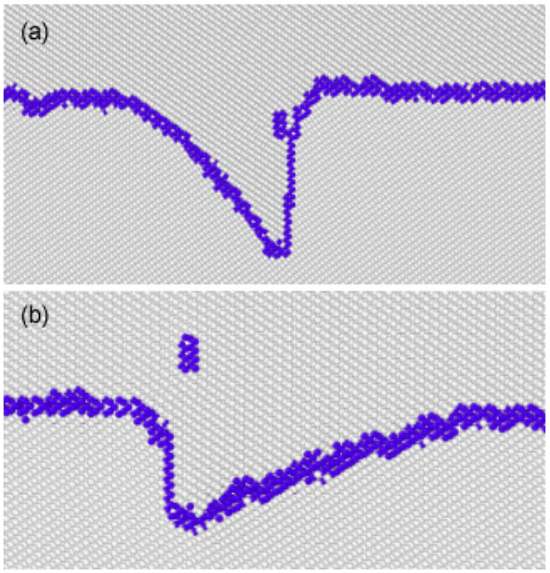

FIG. 5. Snapshots of MD simulation of a {111} GB interacting with a pileup of (a) $\mathbf{b}_{3/0}$ (see video 111.mp4 in Supplemental Material [38]) and (b) $\mathbf{b}_{-3/0}$ dislocations in Fe at 300 K. Two interfaces are generated in the interaction region, a coherent {112} GB and (a) a {001}/{110} facet and (b) a {110}/{112} facet.

IV. GRAIN BOUNDARIES VICINAL TO {112} AND {332} INTERFACES

The boundaries vicinal to the {112} show a comparable accommodation as for low angle GBs; i.e., the increase of misorientation from the pristine {112} GB is accommodated by an array of $\mathbf{b}_{1/-1}$ GBDs, leaving segments of pristine {112} boundary between them, as shown in Fig. 6(a). Under a shear

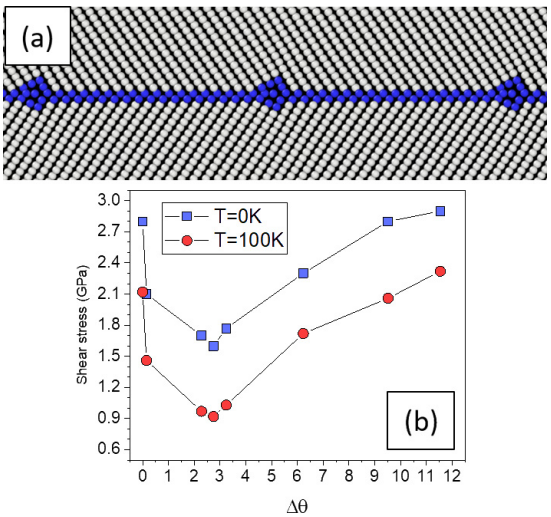

FIG. 6. (a) {112} vicinal GB (19,19,40): $\Delta\Theta = 2.74^\circ$. (b) Resolved shear stress vs increment of misorientation. Includes the pristine {112} GB: $\Delta\Theta = 0^\circ$.

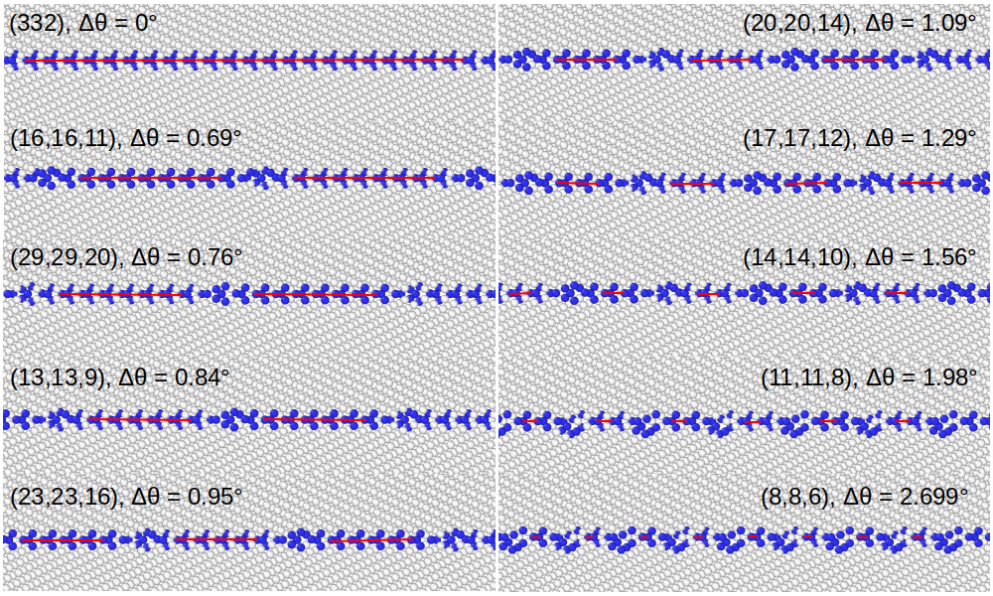

FIG. 7. Snapshots showing the atomic structure of the {332} vicinal GBs investigated. The red lines indicate the location of the pristine {332} segments between the $\mathbf{b}_{1/-1}$ GBDs.

stress, each GBD emits a dipole pair of EDisc (see Fig. 2) that glide up to their annihilation with the neighbor pair. Thanks to the compensated climb of GBDs, these vicinal GBs can perform efficiently SCGBM, with a shear stress level, which can be significantly lower than for the pristine interface.

The critical resolved shear stress presented in Fig. 6(b) is decreasing for low increment of misorientation because there is an increase of sources of EDisc. The tendency is reversed when the distance between sources is small enough to have mutual interaction. As shown in Fig. 6(b), the shear stress necessary to move the GB diminishes with temperature, but the dependency with the increase of misorientation angle is independent of the temperature, therefore the behavior is related to the distance between GBDs, namely, the density of GBD that defines the vicinal GB. A high degree of simplicity is shown by {112} GBs and the set of vicinal GBs: with only one type of EDisc the family of {112} tilt GBs is capable to perform efficiently SCGBM in a conservative way.

The GBs vicinal to the {332} GB show an accommodation similar to the vicinal of {112}, with arrays of $\mathbf{b}_{1/-1}$ GBDs [shown in Fig. 1(b)] that accommodate the increment of misorientation. Figure 7 show the family of possible vicinal GBs. It is worth noticing that these GBDs are specific of the vicinal GBs and are not obtained as a result of the interaction with crystal dislocations. These GBDs do not act as sources of EDisc. In fact, under shear stress, dipole pairs of EDisc are created in the segments of pristine {332} GB and run in opposite directions towards the $\mathbf{b}_{1/-1}$ GBDs, as indicated in Fig. 8(a).

Unlike the {112} vicinal, the migration mechanism of the {332} vicinal is temperature dependent: for $T < 50$ K, the $\mathbf{b}_{1/-1}$ GBDs stop the glide of EDisc, leading to the formation of an array of {112} twins, as shown in Fig. 8(b). For $T \geqslant 50$ K the EDisc overcome the GBD and annihilate with the EDisc of adjacent segments. Then, the GB is able to perform conservative migration as shown in Fig. 8(c). The stress necessary for the migration diminishes with the temperature, as shown in Fig. 8(d). Thus, for {332} tilt GBs and the set of vicinal GBs there are two different mechanisms to accommodate plastic deformation: either SCGBM or formation of {112} twins.

The results obtained for the twin modes underline the relevance of both the production mechanisms of EDisc and the interaction of these EDisc with other GBDs present at the interface, which can activate alternative ways to accommodate plastic deformation.

The {112} interface and its vicinal GBs perform always SCGBM because the Burgers vectors of the EDisc and GBD are perpendicular and the sum is a crystal dislocation. The reaction does not need atomic diffusion and the GBD, acting as a source of EDisc, follows the GB. In contrast, for the {332} vicinal, the ED dipoles are generated in the pristine interface segments between GBDs, therefore a bigger number of GBDs implies more dipoles to be created and therefore higher total stress to produce them. At $T < 50$ K, the EDisc cannot overcome the barrier created by the GBDs, which leads to the creation of twins [Fig. 8(c)]. However, when the temperature is high enough to overcome the energy barrier the EDisc of opposite sign annihilate, allowing SCGBM in a conservative way [Fig. 8(d)]. Both processes are shown in two videos in Supplemental Material [38].

V. THE {116} GRAIN BOUNDARY

The last GB considered is the $\Sigma 19\{116\}\langle 110\rangle$, which is a symmetric tilt GB with a small-angle misorientation ($\Theta = 26.53°$) and a high GB energy (≈ 1.2 J/m^2). The dichromatic pattern shows the potential candidates of EDisc for this GB [Fig. 1(d)]. Based on the behavior observed in the previous GBs, the $\mathbf{b}_{\pm 3/\pm 3}$ is the more suitable as it is the one with smallest ($\mathbf{b}$, h) values (see Table I), although its resolved shear stress (between 4 and 4.7 GPa) is remarkably higher than for $\mathbf{b}_{\pm 1/\pm 1}$ at the {112} (≈ 20 MPa) and $\mathbf{b}_{\pm 2/\pm 2}$ at the {332} (between 550 and 620 MPa). Nonetheless, more types of glissile

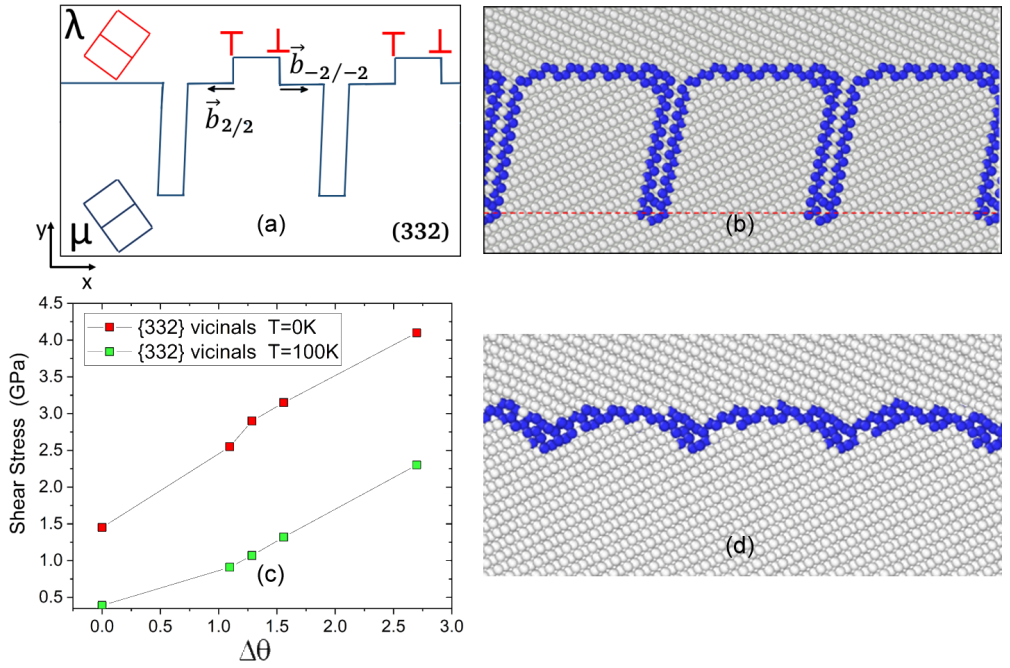

FIG. 8. (a) Schematic showing the SCGBM process by creation of ED dipoles at the pristine segments of the interface. (b, d) Snapshots of the (17,17,12) vicinal of the {332} GB, showing the creation of {112} twins at the $\mathbf{b}_{1/-1}$ GBD positions during the GB migration at $T = 0$ K (see video 171712at0K.mp4 in Supplemental Material [38]) and conservative migration at $T = 100$ K (see video 171712at100K.mp4 in Supplemental Material [38]). The red line indicates the starting location of the GB. (c) Shear stress necessary for the displacement of {332} GBs vs the increment of the misorientation angle.

disconnection appear despite having larger BV and/or higher step height [tagged as $\mathbf{b}_{\pm5/\pm5}$, $\mathbf{b}_{\pm8/\pm8}$, and $\mathbf{b}_{\pm11/\pm11}$ in Fig. 1(d)]. But, at the same time, these high-stepping disconnections (HSDs) are unstable and eventually split in pairs of $\mathbf{b}_{3/3}$ and $\mathbf{b}_{-3/-3}$. For this reason, the {116} GB can be considered as an intermediate case between the {112} and {332} GBs, where only one ED participates in SCGBM and the {111} GB where no EDisc are present, preventing the sustained migration of this interface.

In the case of the pristine interface, SCGBM starts when the shear stress is around 6.6 GPa, by inducing the creation of $\mathbf{b}_{3/3}$ and $\mathbf{b}_{-3/-3}$ pairs. The outcome of the interaction between this GB and crystal dislocations is a GBD along with the emission of ED $\mathbf{b}_{\pm3/\pm3}$. When the local stress on the vicinity of the GBD is high enough then it splits into a new GBD and a HSD, shown in Fig. 9, which in turn ends by splitting into $\mathbf{b}_{3/3}$ and $\mathbf{b}_{-3/-3}$ EDisc. Specifically the crystal dislocation denoted as $\mathbf{b}_{4/0}$ in Fig. 1(d) reacts with the GB as indicated in Fig. 9.

The first step of the reaction is

$$\mathbf{b}_{4/0} = \mathbf{b}_{7/3} + \mathbf{b}_{-3/-3}. \tag{1.1}$$

In Miller indices the reaction is

$$\tfrac{1}{2}[1\bar{1}\bar{1}] = \tfrac{1}{38}[13\ \bar{1}3\ \bar{2}1] + \tfrac{1}{19}[3\bar{3}1]. \tag{1.2}$$

In turn, the disconnection $\mathbf{b}_{7/3}$ decomposes as

$$\mathbf{b}_{7/3} = \mathbf{b}_{-3/-3} + \mathbf{b}_{2/-2} + \mathbf{b}_{8/8}. \tag{2.1}$$

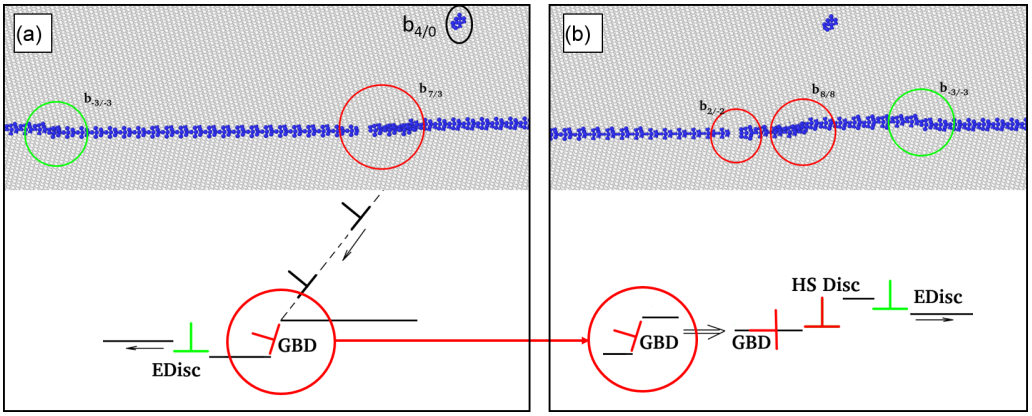

FIG. 9. Snapshots of MD simulation of a (116) GB interacting with a crystal dislocation $\mathbf{b}_{4/0}$ in Fe at 300 K. A second crystal dislocation is shown in the top of the image. (a) First step of the reaction. (b) Decomposition of the $\mathbf{b}_{7/3}$ disconnection.

In Miller indices the reaction is

$$\tfrac{1}{38}[13\ \bar{1}3\ \bar{2}1] = \tfrac{1}{19}[3\bar{3}1] + \tfrac{2}{19}[1\bar{1}\bar{6}] + \tfrac{1}{38}[3\bar{3}1]. \qquad (2.2)$$

The several reactions analyzed indicate that these HSDs, although they show a very short lifetime, seem to play the role of facilitators, allowing a more efficient way to couple plastic deformations by creating new interfacial defects and EDisc capable to sustain SCGBM.

VI. SUMMARY AND CONCLUDING REMARKS

The accommodation of plastic deformation by shear-coupled migration of symmetric tilt GBs in bcc metals is efficiently produced by the glide of disconnections, the description of which is summarized as follows.

The conservative displacement of {112} and {332} symmetric ⟨110⟩ tilt boundaries under shear stress is produced by the motion of EDisc that can be produced either in the pristine GB, as dipole pairs, or by GB dislocations acting as sources of disconnections.

The resolved shear stress of EDisc at the {112} interface is small (about 20 MPa in Fe) and there are no shuffles during glide. This compares with the resolved shear stress of EDisc in the {332} interface ($\approx$ 550–620 MPa in Fe) that requires shuffling an atom at the core of the disconnection during glide to restore the crystal structure. These properties are applicable to the coherent interfaces of the {112} and {332} conjugate twins and they influence the existence of such twins. Whereas the {112} twin is abundant, the {332} twin only appears in some bcc alloys.

These two interfaces are very stable and they form cusps in the curve of the surface energy versus misorientation. Consequently, they can accommodate increments of misorientation up to 11.5° in the {112} GB and 2.7° in the {332} GB by introducing GBDs. The new GBs, named vicinal, are formed by pristine segments separated by GBDs. The {112} vicinal GBs perform shear-coupled GB migration by the glide of the EDisc. The interaction of the EDisc with the GBDs is a conservative climb. The EDisc gliding in {332} vicinal GBs need to overcome an energy barrier when encountering the GBD. To do so the temperature must be above 50 K. At lower temperature the EDisc pile up at the GBD, creating {112} twins.

The Σ19{116} GB presents more than one ED although only one of them is stable and contributes to the displacement of the GB. The level of stress needed to create the EDisc in this GB is much higher than in the {112} and {332} GBs. The other EDisc are produced during the interaction of the GB with crystal dislocations. Although they show a very short lifetime, they seem to play the role of facilitators, allowing a more efficient way to couple plastic deformations by creating new interfacial defects and EDisc capable to sustain the displacement of the GB.

Finally, no EDisc are created at the {111} GB. Under local stress the GBs reorient into a new interface containing {001}/{110} or {110}/{112} facets by pure shuffle of two atoms of the CSL unit cell. This GB is a strong barrier for the glide of crystal dislocations and does not perform shear-coupled GB migration.

ACKNOWLEDGMENTS

This work has received funding from the Euratom research and training programme 2014-2018 under Grant Agreement No. 755039 (M4F project). This work also contributes to the Joint Program on Nuclear Materials of the European Energy Research Alliance.

[1] P. M. Anderson, J. P. Hirth, and J. Lothe, *Theory of Dislocations*, 3rd ed. (Cambridge University, Cambridge, England, 2017).
[2] E. Hall, Proc. Phys. Soc. B **64**, 747 (1951).
[3] A. Rajabzadeh, F. Mompiou, S. Lartigue-Korinek, N. Combe, M. Legros, and D. A. Molodov, Acta Mater. **77**, 223 (2014).
[4] N. Combe, F. Mompiou, and M. Legros, Phys. Rev. Materials **1**, 033605 (2017).
[5] N. Combe, F. Mompiou, and M. Legros, Phys. Rev. Materials **3**, 060601(R) (2019).
[6] W. Z. Abuzaid, M. D. Sangid, J. D. Carroll, H. Sehitoglu, and J. Lambros, J. Mech. Phys. Solids **60**, 1201 (2012).
[7] D. A. Spearot, K. I. Jacob, and D. L. McDowell, Acta Mater. **53**, 3579 (2005).
[8] J. Wang, J. P. Hirth, and C. N. Tomé, Acta Mater. **57**, 5521 (2009).
[9] A. Rajabzadeh, M. Legros, N. Combe, F. Mompiou, and D. A. Molodov, Philos. Mag. **93**, 1299 (2013).
[10] K. D. Molodov, T. Al-Samman, D. A. Molodov, and S. Korte-Kerzel, Acta Mater. **134**, 267 (2017).
[11] H. Khater, A. Serra, R. C. Pond, and J. P. Hirth, Acta Mater. **60**, 2007 (2012).
[12] N. Kvashin, P. L. García-Müller, N. Anento, and A. Serra, Phys. Rev. Materials **4**, 073604 (2020).
[13] N. Kvashin, N. Anento, D. Terentyev, A. Bakaev, and A. Serra, Phys. Rev. Materials **5**, 013605 (2021).
[14] N. Kvashin, A. Ostapovets, N. Anento, and A. Serra, Comput. Mater. Sci. **196**, 110509 (2021).
[15] N. Kvashin, N. Anento, D. Terentyev, and A. Serra, Phys. Rev. Materials **6**, 033606 (2022).
[16] N. Kvashin, N. Anento, D. Terentyev, and A. Serra, Comput. Mater. Sci. **203**, 111044 (2022).
[17] H. Beladi and G. S. Rohrer, Acta Mater. **61**, 1404 (2013).
[18] H. Beladi and G. S. Rohrer, Metall. Mater. Trans. A **44**, 115 (2013).
[19] A. G. Crocker, Acta Metall. **10**, 113 (1962).
[20] H. Tobe, H. Y. Kim, T. Inamura, H. Hosoda, and S. Miyazaki, Acta Mater. **64**, 345 (2014).
[21] J. W. Christian and S. Mahajan, Prog. Mater. Sci. **39**, 1 (1995).
[22] J. Wang, Z. Zeng, C. R. Weinberger, Z. Zhang, T. Zhu, and S. X. Mao, Nat. Mater. **14**, 594 (2015).
[23] R. C. Pond and D. S. Vlachavas, Proc. R. Soc. A **386**, 95 (1983).
[24] R. C. Pond, *Dislocations in Solids* (Elsevier, Amsterdam, 1989), Vol. 8, p. 1.
[25] J. P. Hirth, J. Phys. Chem. Solids **55**, 985 (1994).
[26] J. P. Hirth and R. C. Pond, Acta Mater. **44**, 4749 (1996).

[27] J. Hirth, R. Pond, and J. Lothe, Acta Mater. **55**, 5428 (2007).
[28] S. Plimpton, J. Comput. Phys. **117**, 1 (1995).
[29] G. Ackland, M. I. Mendelev, D. J. Srolovitz, S. Han, and A. V. Barashev, J. Phys.: Condens. Matter **16**, S2629 (2004).
[30] D. Terentyev, X. He, A. Serra, and J. Kuriplach, Comput. Mater. Sci. **49**, 419 (2010).
[31] L. E. Shilkrot, R. E. Miller, and W. A. Curtin, J. Mech. Phys. Solids **52**, 755 (2004).
[32] D. Terentyev, A. Bakaev, A. Serra, F. Pavia, K. L. Baker, and N. Anento, Scr. Mater. **145**, 1 (2018).
[33] A. Stukowski, Modelling Simul. Mater. Sci. Eng. **18**, 015012 (2010).
[34] X. Li, Y. Wei, L. Lu, K. Lu, and H. Gao, Nature (London) **464**, 877 (2010).
[35] M. A. Tschopp, K. N. Solanki, F. Gao, X. Sun, M. A. Khaleel, and M. F. Horstemeyer, Phys. Rev. B **85**, 064108 (2012).
[36] H. A. Khater, A. Serra, and R. C. Pond, Philos. Mag. **93**, 1279 (2013).
[37] N. Anento and A. Serra, Comput. Mater. Sci. **179**, 109679 (2020).
[38] See Supplemental Material at http://link.aps.org/supplemental/10.1103/PhysRevMaterials.6.053607 for videos showing conservative migration of the {112} GB with the GBD acting as a source of ED, formation of new interfaces at the reaction between the DPU and {111} GB, (17,17,12) vicinal of the {332} GB under applied strain showing the creation of {112} twins at the GBD positions during the GB migration at $T = 0$ K, and (17,17,12) vicinal of the {332} GB under applied strain showing the conservative migration at $T = 100$ K.